SOLITONS

Dark photovoltaic spatial solitons in a planar waveguide obtained by proton implantation in lithium niobate

V.G. Kruglov, V.M. Shandarov, Yang Tan, Feng Chen, D. Kip

Abstract. **A photovoltaic dark spatial soliton is generated in a planar waveguide produced by the implantation of protons into a copper-doped lithium niobate crystal. Stationary soliton regimes are achieved at powers 90 and 30 μW at wavelengths 633 and 532 nm, respectively.**

Interest in spatial optical solitons is related to a considerable extent to the fact that they can induce waveguide elements admitting optical erasure and reconfiguration [1]. The possibility of generating spatial solitons at light powers at the microwatt level in photorefractive crystals, predicted in paper [2], was soon confirmed experimentally for strontium – barium niobate (SBN) [3], bismuth titanate [4], potassium niobate [5], and lithium niobate (LiNbO$_3$) [6] crystals. Most of the experimental and theoretical studies in this field [1, 7 – 9] are devoted to spatial solitons inside media. At the same time, of special interest are soliton effects in photorefractive planar waveguides. The existence of modes of different orders with different polarisations and the spatial inhomogeneity of nonlinear optical properties in waveguide structures lead to the difference in the soliton formation time and the storage time of the waveguide elements induced by them upon excitation of solitons by different modes. These features were observed in experiments on the generation of spatial solitons in planar waveguides produced by ion implantation in SBN [10] and the diffusion of Fe and Ti in LiNbO$_3$ [11, 12], and also in the analysis of characteristics of dark photovoltaic solitons in a planar Z-cut Fe : LiNbO$_3$ waveguide [13]. In multimode waveguides, multicomponent spatial solitons can also exist, which have no analogues in bulky media.

The photorefractive properties of optical waveguides considerably depend on their manufacturing technology. Thus, the nonlinear response rate in Fe : LiNbO$_3$ wave-

V.G. Kruglov, V.M. Shandarov Tomsk State University of Control Systems and Radioelectronics, prosp. Lenina 40, 634050 Tomsk, Russia; e-mail: shan@svch.rk.tusur.ru;
Yang Tan, Feng Chen School of Physics, Shandong University, Jinan 250100, People's Republic of China;
D. Kip Institute of Physics and Physical Technologies, Clausthal University of Technology, Clausthal-Zellerfeld, 38678, Germany

guides can be varied by seven – eight orders of magnitude by changing the Fe concentration [11, 14]. The implantation of He$^+$ ions also considerably affects the photorefractive characteristics of SBN [10]. The method of ion implantation provides especially reliable control of the waveguide parameters and opens up wide possibilities for varying the properties of materials in the waveguide region by changing the ion beam energy, the type and dose of implanted ions [15 – 17]. The combination of ion implantation with doping materials by special impurities can significantly broaden the range of possible parameters of generated waveguide spatial solitons, which is important for their practical applications.

In this paper, we demonstrated for the first time the regime of dark photovoltaic spatial solitons in a planar waveguide obtained by the implantation of protons into a Cu : LiNbO$_3$ crystal doped with Cu ions during the crystal growth.

Planar waveguides were formed in X-cut Cu : LiNbO$_3$ plates (with the molar concentration of copper of 0.1%) of size 1.5, 19, and 10 mm along the x, y, and z axes, respectively. The optical-quality-polished yz surface was irradiated by a 500-keV proton beam up to the dose of 1×10^{17} cm^{-2}. Then, the plates were annealed at 400 °C for 30 min in air to remove point stresses and relaxation of colour centres appearing in the waveguide region during implantation. The polishing quality of the xz plate surface provided the coupling of light through the waveguide end. The mode composition and optical losses of waveguides were studied with the help of a prism coupling element, while refractive index profiles were reconstructed by using the TRIM (Transport and Ranges of Ions in Matter) standard program [16]. The inset in Fig. 1 shows the profile of the extraordinary refractive index $n_e(x)$. The two TE modes with the effective refractive indices $n_0 = 2.2033$ and $n_1 = 2.1988$ are excited at a wavelength of 532 nm (TM modes are not supported in H$^+$: LiNbO$_3$ waveguides). The TE$_1$ mode is a radiation mode. For this mode, $n_1 < n_s$ (the refractive index of the substrate is $n_s = 2.201$). The radiation loss at 633 nm for the TE$_0$ mode propagating along the y axis does not exceed 1 dB cm^{-1}, while this loss for the TE$_1$ mode exceeds 20 dB cm^{-1} due to radiation through the barrier layer to the substrate. The waveguide layer thickness is ~ 3.5 μm.

The scheme of the experimental setup is shown in Fig. 1. Radiation sources are a 633-nm He – Ne laser and a frequency-doubled 532-nm cw Nd^{3+} : YAG laser. The polarisation of light corresponds to the extraordinary wave in the crystal, and dark solitons can be formed and waveguides channels induced by them can be read out by
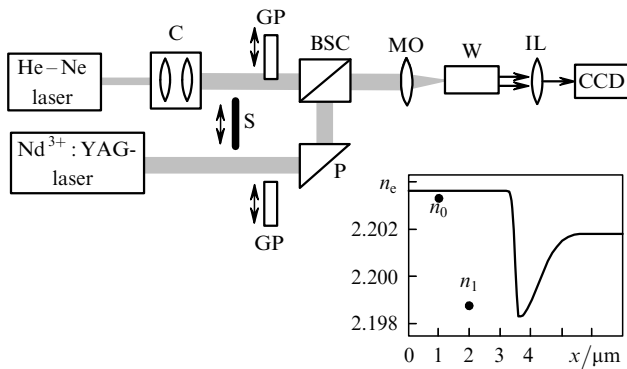
Figure 1. Scheme of the experimental setup and profile of the extraordinary refractive index of the waveguide: (C) collimator; (GP) glass plate; (P) prism; (BSC) beamsplitter cube; (S) shutter blocking beams; (MO) microobjective; (W) waveguide; (IL) imaging lens.

radiation at the same of different wavelengths. The diameters of the light beams are equalised with the help of collimator C and their coaxial propagation is adjusted with the help of prism P and beamsplitter cube BSC. Light is focused by microobjectives MO with the magnification $3.7^{\times}$ or $8^{\times}$ on the end-face of a planar waveguide. To generate dark solitons, light beams with out-of-phase fields in different halves of the aperture are required [6]. We obtained such beams by inserting a thin glass plate GP into the beam, which blocked half its aperture and provided the required phase shift being properly oriented [11]. The image of the output plane of the waveguide is projected on a CCD camera by an imaging lens IL. The glass plate is periodically removed from the beam during the readout time (~ 1 s). This allows us to study the time evolution of the readout beam field caused by the induction of a nonlinear lens by the forming beam. In addition, this lens can be probed by a light

beam at a different wavelength, which is blocked with a shutter S during soliton formation and is 'switched on' during readout, when the forming beam is blocked.

Figure 2 shows the evolution of the fields of the forming and reading beams during the excitation of a dark photovoltaic spatial soliton by the 633-nm beam and read-out of a waveguide channel induced by it at 532 nm. The forming beam with a hole of width (FWHM) ~ 12 μm in the intensity distribution in the input plane of the waveguide and ~ 120 μm in its output plane had the power $P_{in} = 90$ μW, while the readout beam power was ~ 1 μW. Already after $2-5$-min exposures, the hole in the intensity distribution in the output plane was narrowed down and the light field was localised in the readout beam.

For $t = 15 - 18$ min, the diffraction divergence of the readout beam in the waveguide plane was almost completely compensated due to its capture by the channel waveguide induced by the dark soliton field. In the case of the forming beam at 532 nm with $P_{in} = 30$ μW, the soliton regime was achieved for ~ 4 min. The storage time of induced waveguide channels in the absence of a special illumination was a few hours. During continuous readout by light at 532 nm and $P_{in} = 1 - 100$ μW, a channel waveguide induced by a soliton was 'erased' for the time from $10-20$ min to a few seconds.

Figure 3 demonstrates the dependences of the readout beam width in the output plane of the waveguide on the readout time for $P_{in} = 20$ and 1 μW. The storage time of the induced waveguide cannels proved to be considerable shorter than that for photorefractive gratings in the $Cu:LiNbO_3$ substrate, which is explained by the increase in the conductivity of the material in the barrier layer due to implantation (this effect was earlier observed in ion-implanted SBN waveguides [10]).

Thus, we have demonstrated experimentally the generation of dark photovoltaic spatial solitons by light beams
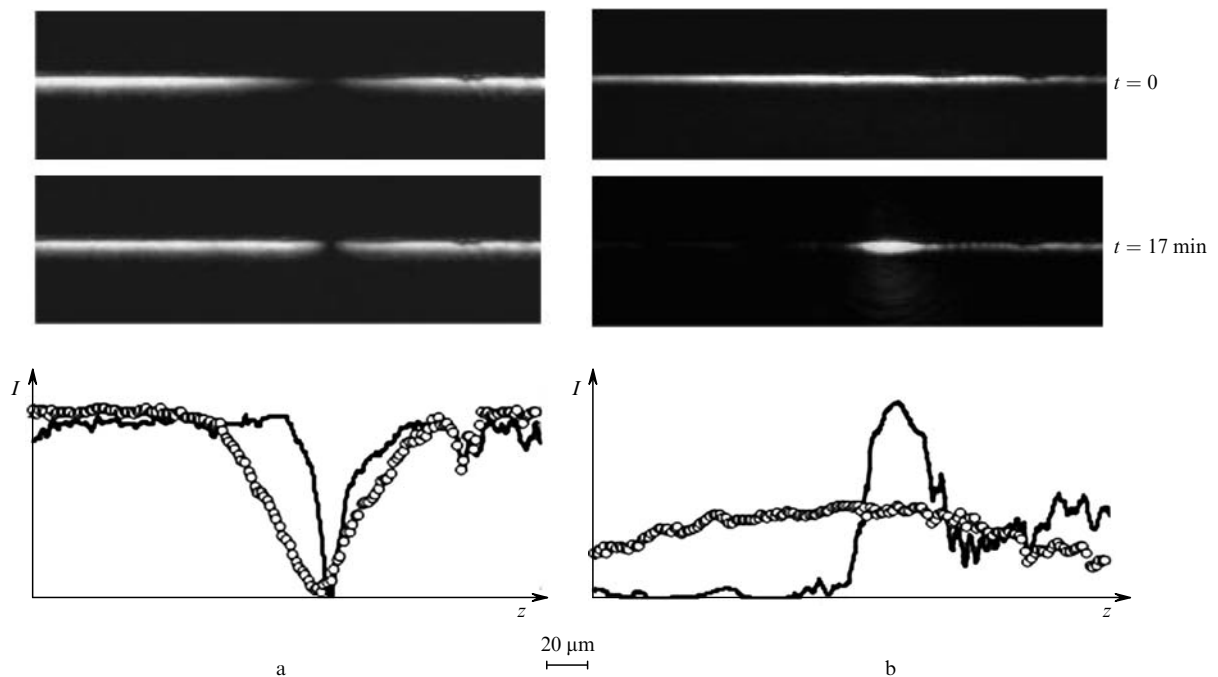

Figure 2. Light field intensity distributions and corresponding intensity profiles of the forming (a) and readout (b) beams in the output plane of the waveguide in the linear regime ($t = 0$, circles) and in the dark spatial soliton regime ($t = 17$ min, solid curves).
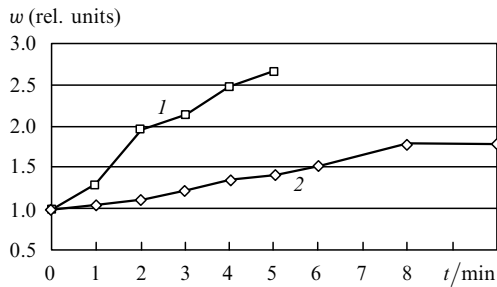
Figure 3. Dependences of the readout beam FWHM w in the output plane of the waveguide on the readout time of the waveguide channel induced by a dark soliton for $\lambda = 532$ nm, $P_{in} = 20$ (*1*) and 1 μW (*2*).

of power a few tens of microwatts in a proton-implanted planar Cu : LiNbO$_3$ waveguide. We have also shown that the waveguide channels induced by solitons can be promptly optically erased.

References

1. Stegeman G.I., Segev M. *Science*, **286**, 1518 (1999).
2. Segev M., Crosignani B., Yariv A., Fischer B. *Phys. Rev. Lett.*, **68**, 923 (1992).
3. Duree G., Shultz J., Salamo G., Segev M., Yariv A., Crosignani B., DiPorto P., Sharp E., Neurgaonkar R.R. *Phys. Rev. Lett.*, **71**, 533 (1993).
4. Iturbe-Castillo M.D., Marquez-Aguilar P.A., Sanchez-Mondragon J.J., Stepanov S., Vysloukh V. *Appl. Phys. Lett.*, **64**, 408 (1994).
5. Lan S., Shih M., Segev M. *Opt. Lett.*, **22**, 1467 (1997).
6. Taya M., Bashaw M., Fejer M., Segev M., Valley G.C. *Phys. Rev. A*, **52**, 3095 (1995).
7. Segev M., Valley G.C., Bashaw M.C., Taya M., Fejer M.M. *J. Opt. Soc. Am. B*, **14**, 1772 (1997).
8. Shih M.-F., Chen Z., Mitchell M., Segev M., Lee H., Feigelson R.S., Wilde J.P. *J. Opt. Soc. Am. B*, **14**, 3091 (1997).
9. Christodoulides D.N., Carvalho M.I. *J. Opt. Soc. Am. B*, **12**, 1628 (1995).
10. Kip D., Wesner M., Shandarov V., Moretti P. *Opt. Lett.*, **23**, 921 (1998).
11. Shandarov V., Kip D., Wesner M., Hukriede J. *J. Opt. A: Pure Appl. Opt.*, **2**, 500 (2000).
12. Chauvet M., Chauvin S., Maillotte H. *Opt. Lett.*, **26**, 1344 (2001).
13. Frolova M.N., Borodin M.V., Shandarov S.M., Shandarov V.M., Larionov Yu.M. *Kvantovaya Elektron.*, **33**, 41 (2003) [*Quantum Electron.*, **33**, 41 (2003)].
14. Kip D. *Appl. Phys. B*, **67**, 131 (1998).
15. Chen F., Hu H., Wang X.L., Lu F., Wang K.M. *J. Appl. Phys.*, **98**, 044507 (2005).
16. Kip D., Aulkemeyer S., Moretti P. *Opt. Lett.*, **20**, 1256 (1995).
17. Ramabadran U.B., Jackson H.E., Boyd J.T. *Appl. Opt.*, **32**, 313 (1993).